Asphaltene Thermodynamic Flocculation during Immiscible Nitrogen Gas Injection

Mukhtar Elturki and Abdulmohsin Imqam*, Missouri University of Science and Technology

Summary

Gas-enhanced oil recovery is one of the most advantageous enhanced oil recovery methods. Nitrogen is one of the most investigated gases because of its beneficial properties. However, during its interaction with crude oil, nitrogen can induce asphaltene deposition, which may result in severe formation damage and pore plugging. Few works have investigated the impact of nitrogen on asphaltene instability. This research studied the immiscibility conditions for nitrogen in nanopores and the impact of nitrogen on asphaltene precipitations, which could lead to plugging pores and oil recovery reduction. A slimtube was used to determine the minimum miscibility pressure (MMP) of nitrogen to ensure that all the experiments would be carried out below the MMP. Then, filtration experiments were conducted using nanofilter membranes to highlight the impact of the asphaltene particles on the pores of the membranes. A special filtration vessel was designed and used to accommodate the filter paper membranes. Various factors were investigated, including nitrogen injection pressure, temperature, nitrogen mixing time, and pore size heterogeneity. Supercritical phase nitrogen was used during all filtration experiments. Visualization tests were implemented to observe the asphaltene precipitation and deposition mechanism over time. Increasing the nitrogen injection pressure resulted in an increase in the asphaltene weight percent in all experiments. Decreasing the pore size of the filter membranes resulted in an increase in the asphaltene weight percent. Greater asphaltene weight percents were observed with a longer nitrogen mixing time. Visualization tests revealed that asphaltene clusters started to form after 1 hour and fully deposited after 12 hours in the bottom of the test tubes. Chromatography analysis of the produced oil confirmed that there was a reduction in the heavy components and asphaltene weight percent. Microscopy and scanning electron microscopy (SEM) imaging of the filter paper membranes found that significant pore plugging resulted from asphaltene deposition and precipitation. This research investigated asphaltene precipitation and deposition during immiscible nitrogen injection to understand the main factors that impact the success of using such a technique in unconventional shale reservoirs.

Introduction

Gas-injection-enhanced oil recovery methods have been investigated in unconventional reservoirs, with the results showing an increase in oil recovery. Experimental studies have indicated a positive result in increasing oil recovery from shale cores using cyclic nitrogen and carbon dioxide injection (Gamadi et al. 2013; Yu and Sheng 2015). Injection of carbon dioxide and nitrogen mixtures has been also studied for storing carbon dioxide and increasing hydrocarbon production from unconventional resources (Hassanpouryouzband et al. 2018; 2019). However, injection of a gas changes the equilibrium conditions and fluid properties of the oil in the reservoir. Changing the equilibrium may lead to instability in the colloidal suspension, manifested by asphaltene precipitation and flocculation. Carbon dioxide and nitrogen could cause a different degree of asphaltene flocculation into the reservoir. Carbon dioxide has good solubility in crude oil and can easily attain a supercritical condition in reservoir conditions (Wang et al. 2018). Thus, the mass transfer ability of supercritical carbon dioxide is strong. In the carbon dioxide injection process, the carbon dioxide-crude oil system could easily reach a miscible or near-miscible state that enhances and extracts the light hydrocarbon components from crude oil into the gas phase. At similar thermodynamic conditions, nitrogen has weaker solubility in crude oil than carbon dioxide. Nitrogen has a weak mass transfer capacity, which could lead to the poor extraction of light hydrocarbons and probably less asphaltene flocculation compared to carbon dioxide (Chung 1992; Wang et al. 2018). Asphaltene is the heaviest component that occurs in petroleum fluids and that is insoluble in light n-alkanes, such as n-pentane or n-heptane. However, asphaltene is soluble in aromatics, such as toluene or benzene (Goual and Firoozabadi 2002). Asphaltene, a solid component of crude oil, has an extremely high molecular weight (Mozaffari et al. 2015). Under reservoir temperature and pressure conditions, asphaltene can be in solution or in a colloidal suspension (Jamaluddin et al. 2002). Asphaltene instability can be induced when the injection of carbon dioxide, nitrogen, and hydrocarbon gases changes the solubility of the reservoir fluids (Yang et al. 1999; Dahaghi et al. 2008; Moradi et al. 2012a; Shen and Sheng 2016; Fakher et al. 2020a). When the solid phase is formed after the liquid phase, precipitation occurs. The deposition is the adherence of the solid phase to the reservoir rocks (Zendehboudi et al. 2014). This is the fundamental cause of problems related to asphaltene deposition and precipitation, in which asphaltene becomes denser in the reservoir, production facilities, and transportation pipelines. Understanding the behavior and the factors that affect asphaltene deposition and precipitation is crucial because of the additional economic costs that must be incurred to solve the aforementioned asphaltene deposition issues.

Recently, the effects of asphaltene deposition on enhanced oil recovery have gained more attention because of its impact on production processes and its deposition resulting in lower oil recovery. Many studies have investigated asphaltene deposition and have aimed to improve shale recoveries during carbon dioxide injection (Alta'ee et al. 2012; Ren et al. 2011). However, there is a lack of nitrogen immiscible injection research in the oil industry (Necmettin 2003; Jamaluddin et al. 2002; Zadeh et al. 2011; Moradi et al. 2012a; Buriro and Shuker 2012, 2013; Elwegaa and Emadi 2019; Mansoori and Elmi 2010; Hajizadeh et al. 2009; Fakher et al. 2019a, 2020b; Khalaf and Mansoori 2019; Elturki and Imqam 2020a, 2021). Fakher et al. (2020b) investigated asphaltene deposition and pore plugging in nanopores during carbon dioxide injection and evaluated the main factors that impact asphaltene deposition. The results showed that increasing the injection pressure of carbon dioxide resulted in increased asphaltene in the produced oil. Conversely, increasing the temperature reduced the amount of asphaltene in the produced oil. Elwegaa and Emadi (2019) conducted an experiment using cold nitrogen via cyclic gas injection in shale cores. The results demonstrated a higher recovery factor when the pressure increased using the cold nitrogen injection. Jamaluddin et al. (2002) stated that asphaltene instability was aggravated by nitrogen injection, and the bulk

Original SPE manuscript received for review 9 March 2021. Revised manuscript received for review 21 April 2021. Paper (SPE 206709) peer approved 5 May 2021.

 $[\]hbox{*Corresponding author; email: aimqam@mst.edu}\\$

Copyright © 2021 Society of Petroleum Engineers

precipitation amount was increased by elevating the concentration of nitrogen in the reservoir fluids. Zadeh et al. (2011) examined the effect of nitrogen on asphaltene instability by combining 10 mol% of nitrogen with the target oil at a reservoir temperature of 240°F. Because of the low asphaltene content of the target oil, the asphaltene precipitation was not clearly detected, and the nitrogen mol% was increased in the second sample. Zadeh et al. (2011) also investigated the effect of a lower temperature than 240°F, finding that asphaltene became more unstable as the temperature increased when the pressure was greater than the bubblepoint. Moradi et al. (2012a) studied asphaltene particle precipitation, aggregation, and breakup using natural depletion and miscible nitrogen injection processes. Using high-pressure filtration, it was observed that nitrogen injection stabilized asphaltenes. Moreover, the study highlighted that the problems were more severe in heavier crude oil.

The negative effects of asphaltene deposition and precipitation on plugging pores are much more prevalent in unconventional reservoirs. Shale pore and throat sizes are usually much smaller than those in conventional reservoirs (Elturki and Imqam 2020b). Maroudas (1966) concluded that particles that have a size greater than one-third of pores sizes would block the pores and throats. When asphaltene particles are destabilized in solution, asphaltene flocculation occurs and can cause severe problems. Moradi et al. (2012b) conducted an experiment using nitrogen and methane with a 0.2-µm-pore size filter membrane and reported that asphaltene deposition was much higher in methane than in nitrogen. However, very few studies have been conducted to investigate asphaltene instability in crude oil during nitrogen injection in nanopore-sized features, such as unconventional shale reservoirs. The ultimate goal of this research is to highlight the severity of asphaltene damage during nitrogen gas injection, especially in nanopore structures, which are mainly present in unconventional reservoirs. By studying the impact of different factors on asphaltene formation damage, asphaltene deposition may be mitigated in future applications of nitrogen injection.

Asphaltene Deposition and Precipitation

Multiple compounds can be found in crude oil, depending on its composition. These compounds can be found in three phases: gases, liquids, and solids. The liquid phase consists of saturates, aromatics, and resins. Asphaltenes are the most common solids that exist in crude oil (Fakher et al. 2020b). Asphaltenes are the main polar components of crude oil, and they contain heteroatoms, such as nitrogen, sulfur, or oxygen, which can be soluble in aromatic solvents but insoluble in paraffinic liquids (Goual and Firoozabadi 2002; Speight 2014; Nguyen et al. 2020). However, saturates and aromatics are nonpolar compounds. Resins can be a good bridging agent to hold the polar and nonpolar components because resins have both polar and nonpolar sites (Fakher and Imqam 2019). Fig. 1 shows the main components of crude oil and asphaltene precipitation. Plugging reservoir pores and changing the formation wettability are common issues (Shen and Sheng 2016). Fig. 2 presents formation wettability alterations caused by asphaltene precipitation.

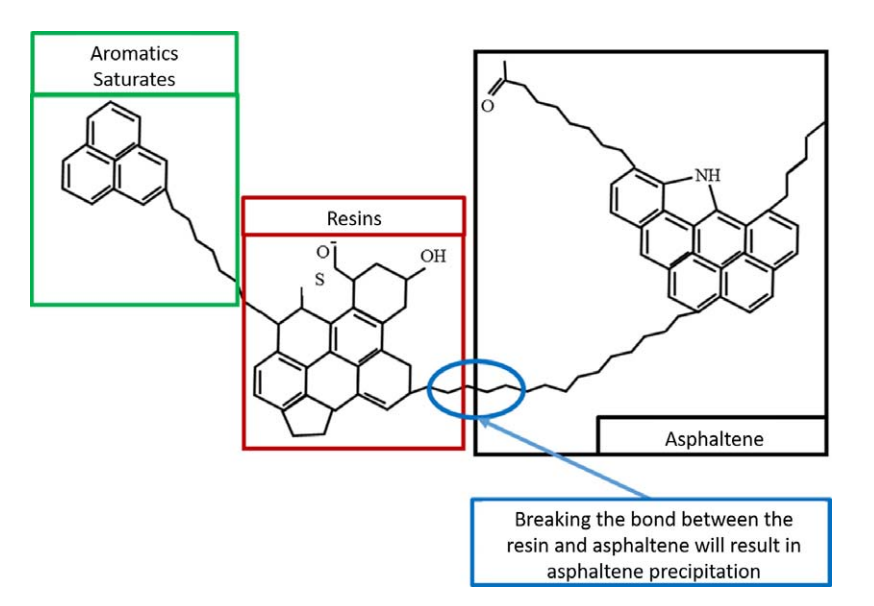


Fig. 1—Main components of crude oil and asphaltene precipitation (Fakher et al. 2019b).

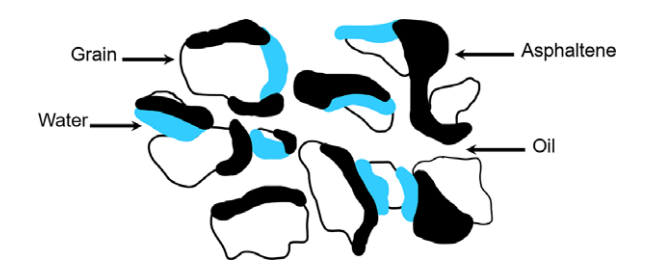


Fig. 2—Formation wettability alterations caused by asphaltene precipitation.

Experimental Test Matrix

Three sets of experiments were conducted: MMP experiments, filtration experiments, and asphaltene visualization experiments, with Fig. 3 displaying an experimental flow chart. First, the MMP of nitrogen was determined to ensure consistent pressure in the filtration experiments under immiscible conditions. Then, the visualization experiments were conducted, followed by asphaltene weight percent calculations.

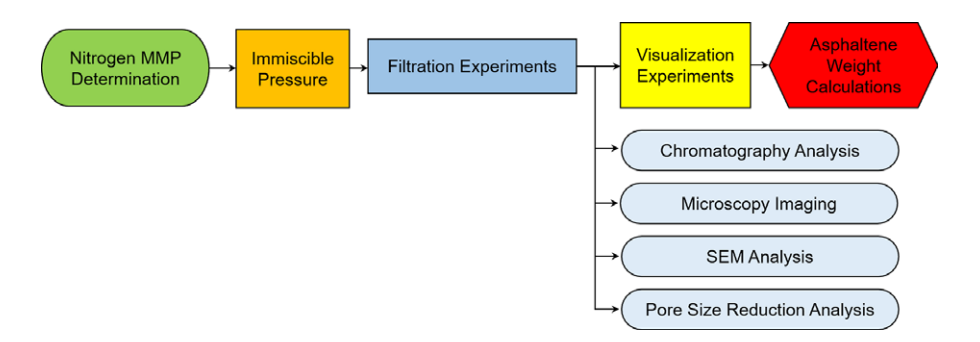


Fig. 3—Experimental design flow chart.

Table 1 presents a description of all of the experiments conducted in this research along with the significant factors they investigated.

	Experiment/ Analysis Type	Factor					
No.		Nitrogen Injection Pressure (psi)	Filter Membrane Pore Size (nm)	Filter Membrane Distribution	Mixing Time	Temperature (°C)	
1	MMP	500 to 2,000	_	_	_	32°C	
2	MMP	500 to 2,000	_	_	_	70°C	
3	Filtration	1,000	450, 100, 50	Heterogenous	2 hours	32°C	
4	Filtration	1,250	450, 100, 50	Heterogenous	2 hours	32°C	
5	Filtration	1,500	450, 100, 50	Heterogenous	2 hours	32°C	
6	Filtration	1,000	100, 100, 100	Uniform	2 hours	32°C	
7	Filtration	1,000	450, 100, 50	Heterogenous	1 hour	32°C	
8	Filtration	1,000	450, 100, 50	Heterogenous	10 minutes	32°C	
9	Filtration	1,000	450, 100, 50	Heterogenous	2 hours	70°C	
10	Visualization	1,000	450, 100, 50	Heterogenous	2 hours	32°C	
11	Visualization	1,000	450, 100, 50	Heterogenous	1 hour	32°C	
12	Visualization	1,000	450, 100, 50	Heterogenous	10 minutes	32°C	
13	Visualization	1,250	450, 100, 50	Heterogenous	2 hours	32°C	
14	Visualization	1,500	450, 100, 50	Heterogenous	2 hours	32°C	
15	Microscope imaging	1,000, 1,250, 1,500	450, 100, 50	Heterogenous	2 hours	32°C	
16	Gas chromatography	1,000, 1,500	_	Heterogenous	_	_	
17	SEM analysis	1,000, 1,500	450, 100, 50	Heterogenous	2 hours	32°C	
18	Pore size distribution	1,000, 1,500	450, 100, 50	Heterogenous	2 hours	32°C	

Table 1—Summary of all experiments conducted in this research.

Experiments Materials. *Crude Oil.* The crude oil had a viscosity of 19 cp, density of 0.864 g/cm³, and API of 32°. The viscosity was measured using a rheometer. Gas chromatography-mass spectrometry was used to determine the composition of the crude oil, as shown in **Table 2.**

Components	Weight Percent (%)		
C ₈ to C ₁₄	65.14		
C ₁₅ to C ₁₉	6.06		
C ₂₀ to C ₂₄	9.16		
C ₂₅ to C ₂₉	14.48		
C_{30+}	5.17		
Total	100.00		
-			

Table 2—Crude oil composition.

Nitrogen. A nitrogen gas cylinder with 99.9% purity was connected to the filtration vessel and used for nitrogen injection, with a pressure regulator controlling the nitrogen cylinder pressure.

Filter Membranes. Various filter membranes (i.e., 50, 100, and 450 nm) were used to investigate the effect of different pore sizes. The membranes were cut to the desired shape based on the 45-mm diameter of the filtration vessel.

Specially Designed High-Pressure, High-Temperature Filtration Vessel. A high-pressure, high-temperature filtration vessel was in particular designed in the laboratory to accommodate the filter paper membranes.

Oven. An oven that accommodated the filtration vessel was used to investigate the effect of various temperatures on asphaltene precipitation and deposition during nitrogen injection.

n-Heptane. A solvent was used to dissolve the oil samples in tubes to quantify the asphaltene weight percent after each experiment. *Slimtube.* A stainless steel slimtube packed with sand was used to determine the MMP of nitrogen.

MMP Experiment. The MMP experiment was conducted to ensure that all subsequent filtration experiments were carried out below the MMP. The MMP can be defined as the lowest pressure at which a gas can create miscibility with the reservoir oil at the reservoir temperature. In other words, the MMP is the lowest pressure at which miscibility between the injected gas and reservoir oil is achieved when the interfacial tension between the oil and gas vanishes after multiple contacts. Fig. 4 shows a schematic of the slimtube experimental setup. The main components of the slimtube test were a syringe pump, three accumulators, gas cylinders, a stainless steel slimtube packed with sand, and a backpressure regulator. The slimtube tests were divided into several steps, starting with the pretest to calculate the pore volume (PV). The second step was to fill the slimtube with the crude oil at a low rate of 0.5 PV to ensure that the slimtube was 100% saturated at the end of pumping. The final step involved experimental manipulation, whereby the temperature was adjusted to a predefined level, the gas cylinder was filled with nitrogen, and gas was injected at a rate of 1.2 PV. A backpressure regulator was installed at the outlet of the slimtube and used to adjust the pressure with another water pump as a backpressure reservoir.

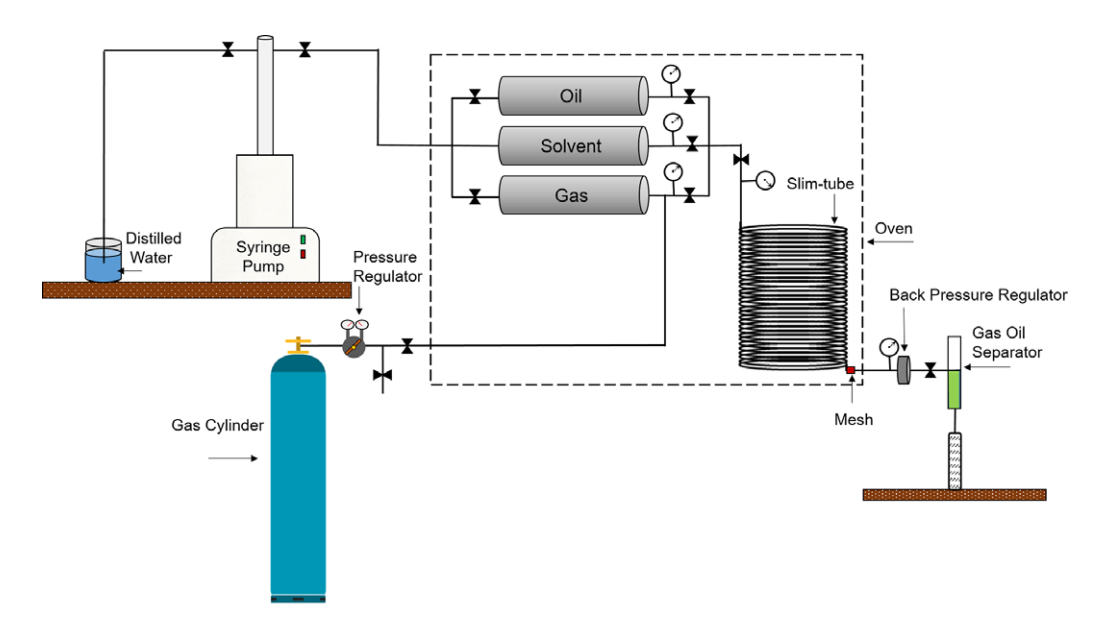


Fig. 4—Slimtube experimental setup.

MMP Experiment Procedure. First, the slimtube was fully saturated with the distilled water. Then, the oil was injected into the slimtube unit fully saturated. This can be observed at the outlet of the slimtube, where the produced liquids are only oil and thus ensure that the slimtube is fully saturated. During all the experiments, the backpressure regulator was placed at the outlet with the desired pressure. The gas accumulator was filled with nitrogen. Then, nitrogen was injected at a rate of 0.25 mL/min. Each experiment was stopped when 1.2 PV of gas was injected or when the gas reached breakthrough. The effluent was used to collect the produced oil. The MMP can be determined by plotting nitrogen injection pressures vs. cumulative oil recoveries. Finally, the solvent of xylene was used after each experiment to clean the slimtube setup and to make sure there was no oil left in the slimtube that could affect the next experiment.

Filtration Experiments. Fig. 5 illustrates all the components of the experimental setup. The main components included a high-purity nitrogen cylinder with a pressure regulator to control the pressure from the cylinder. The filtration vessel was designed to accommodate three mesh screens to support the filter membranes and prevent them from folding under high pressures. The mesh screens were created with small holes that allowed the oil to pass through easily. Spacers between each mesh screen supported the screens in place; rubber O-rings were used above and below each spacer to prevent any leakage and to ensure that the oil and gas would pass through the filter paper membranes. A backpressure regulator was installed at the outlet of the filtration vessel and used to adjust the pressure via a syringe pump. The produced oil was collected using an effluent below the filtration vessel. An oven controlled the temperature of the filtration vessel to study the effect of different temperatures. Finally, two transducers were installed at the inlet and outlet of the filtration vessel and were connected to a computer to monitor and record the pressure difference.

Filtration Experimental Procedure. These steps were followed to conduct the filtration experiments:

- 1. The first set of mesh screens, filter membrane papers, rubber O-rings, and spacers were placed inside the filtration vessel. This step was repeated for the next two sets.
- 2. The vessel was closed tightly using a specially designed cap to ensure that all of the sets remained tightly bound together and to prevent any leakage during the experiment.
- 3. Crude oil (30 mL) was poured into the accumulator, with a syringe pump to inject the oil into the vessel.
- 4. Nitrogen was injected into the cylinder to reach the desired level. The crude oil was then exposed to the gas for a predetermined mixing time.
- 5. After mixing, the syringe pump at the outlet was used at constant pressure. It was adjusted to the required backpressure for each experiment to let the crude oil pass through the membranes.

- 6. Nitrogen was injected into the vessel, and the produced oil was collected. The experiment was stopped when no further oil production was observed.
- 7. The inlet and outlet pressures were observed and recorded using transducers that connected to a computer. The difference between the two pressures did not exceed 50 psi.
- 8. After the gas injection was complete, the vessel was opened, and the remaining crude oil was collected from each filter membrane for asphaltene analysis.

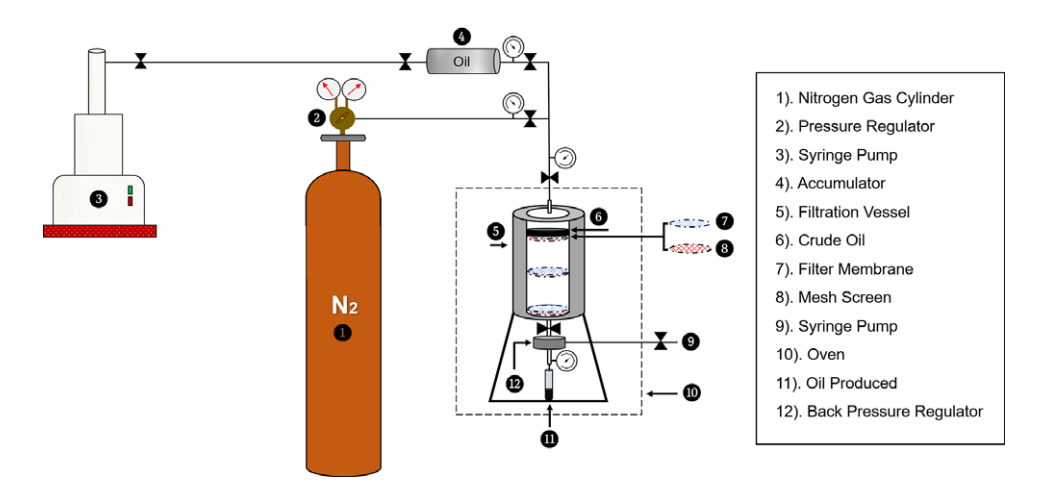


Fig. 5—Filtration experimental setup.

Asphaltene Detection Test and Visualization Experiments Procedure. Asphaltene weight percent can be calculated by weighing the filter paper before and after filtration. The difference between the weights determined the asphaltene percent weight, using the following equation:

$$Asphaltene \ wt\% = \frac{wt_{asphaltene}}{wt_{oil}} * 100, \tag{1}$$

where asphaltene wt% is the asphaltene weight percent, $wt_{asphaltene}$ is the asphaltene weight on the filter paper, and wt_{oil} is the oil sample weight. The asphaltene quantification test procedure can be summarized in the flow chart shown in **Fig. 6**. Photos were taken of the asphaltene precipitation in the test tubes at specific time points (i.e., 0, 2, 4, and 12 hours) to observe the change in asphaltene settling over time.

Results and Discussion

MMP Experiments Results. Nitrogen can achieve miscibility using the same mechanism as carbon dioxide (i.e., the vaporizing mechanism). The nitrogen MMP experiments sought to ensure that the filtration experiments would be conducted under immiscible injection pressure. The effect of temperature on the nitrogen MMP was investigated to ensure that at higher temperatures, the filtration experiments would be less than the MMP. Oil recoveries were recorded at gas breakthrough or at 1.2 PV of the gas injected and were plotted with the tested injection pressures. The MMP can be estimated when the cumulative oil recovery is greater than or equal to 90% of the original oil in place. The solid lines in Fig. 7 were used to determine the sudden slope change point in the measured oil recovery vs. injection pressure. The intersection point can be used to determine the MMP. The MMP of nitrogen at 32°C was 1,600 psi. Hence, 1,000, 1,250, and 1,500 psi along with a temperature of 32°C were selected for investigating asphaltene precipitation under immiscible gas injection conditions. The results also showed that the MMP of nitrogen at 70°C was 1,350 psi. The temperature is inversely proportional to the nitrogen MMP because of the nitrogen remaining in the gaseous phase at the same conditions (Sebastian and Lawrence 1992; Vahidi and Zargar 2007; Belhaj et al. 2013). Thus, the effect of temperature can be investigated because of the immiscible pressure conditions at higher temperatures.

Filtration and Visualization Results. *Effect of Immiscible Pressure Using Uniform Membrane Distribution.* Uniform membrane distribution means that the same pore size of the filter membrane was used in all of the filtration experiments. **Fig. 8** shows the paper membrane distribution inside the vessel, where the entire membrane had a pore size of 100 nm. The selection of filter membrane pore sizes was based on the pore size distribution of shale reservoirs, specifically Eagle Ford (Shen and Sheng 2017).

Fig. 9 displays the effect of using a uniform pore size filter paper membrane on the asphaltene deposition during the filtration test. Three 100-nm filter membranes were placed inside the vessel in each mesh screen to investigate the effect of using the same pore size, and the results were compared with a heterogeneous distribution. Nitrogen pressures of 1,000, 1,250, and 1,500 psi and a temperature of 32°C were used throughout this experiment. The results revealed that the asphaltene deposition was almost equal across all the paper membranes. For instance, the asphaltene weight percent ranged from 5.26% in the upper part of the 100-nm paper membrane to 5.62% in the lower part of the 100-nm paper membrane during the 1,000 psi gas injection. A slightly higher asphaltene weight percent was observed on the upper part of the filter membrane, which could occur because some asphaltene particles plugged some pores, thereby preventing effective oil passage. The asphaltene particles with a size greater than 100 nm precipitated on the upper section of the filter membrane, whereas the particles with a size less than 100 nm passed through to where the produced oil was collected. For example, a pressure of 1,500 psi produced many more asphaltene clusters than did 1,000 psi and also led to more asphaltene being deposited on the filter membranes. The higher pressure resulted in more clusters sized 100 nm or more. Thus, more asphaltenes were quantified at higher pressure levels in all filter membranes. Some of the particles plugged some pores on the middle and lower parts of the filter membrane, as can be observed in the results as slight fluctuations in the asphaltene weight percent. However, these plugged pores resulted in a decrease in the asphaltene weight percent in the produced oil. It can be concluded that the asphaltene was mobilized and forced into the filter membranes with almost the same concentration because of the uniform pore sizes.

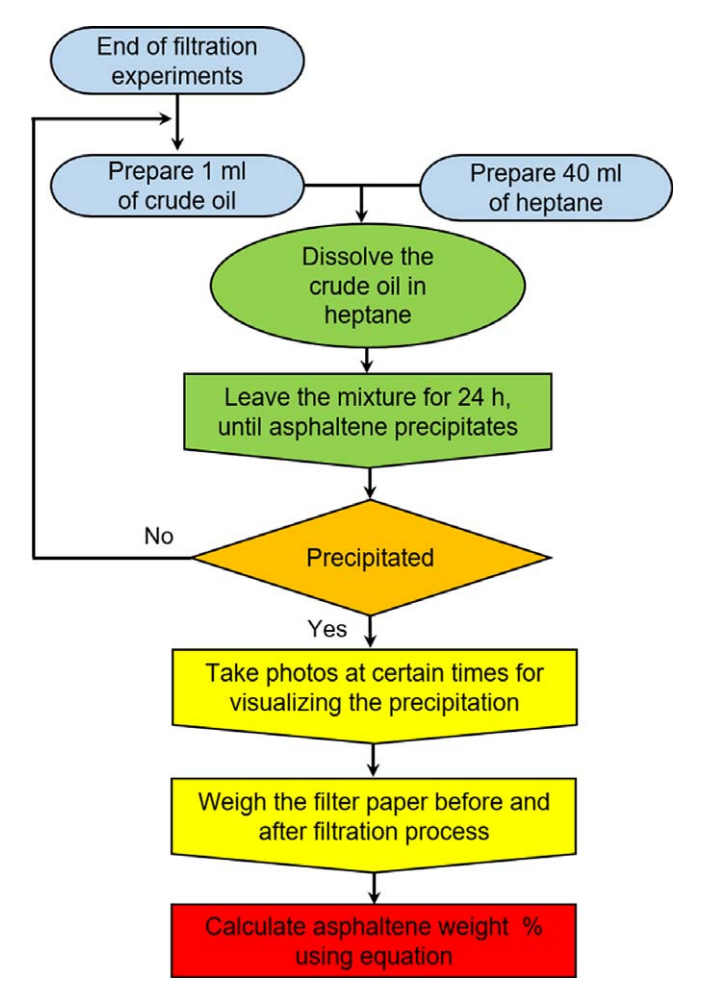


Fig. 6—Flow chart highlighting the main steps of asphaltene quantification.

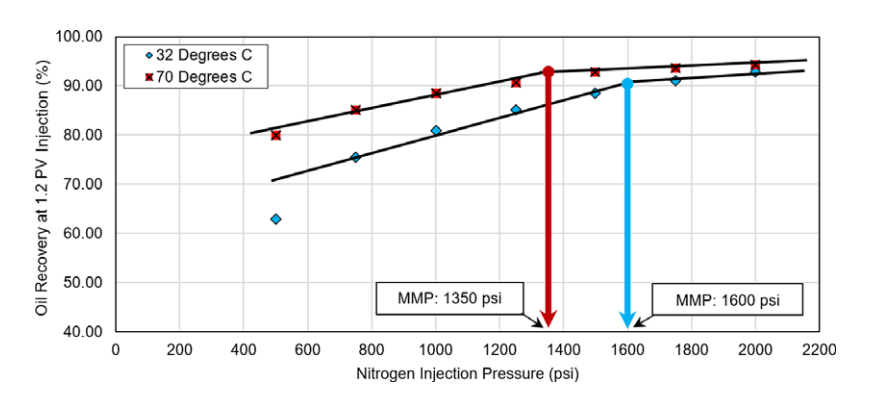


Fig. 7—Nitrogen MMP determination using an oil viscosity of 19 cp at 32 and 70°C.

Uniform Paper Membranes

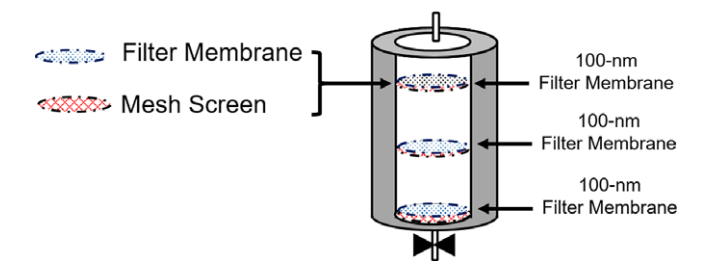


Fig. 8—Uniform paper membrane distributions inside the vessel.

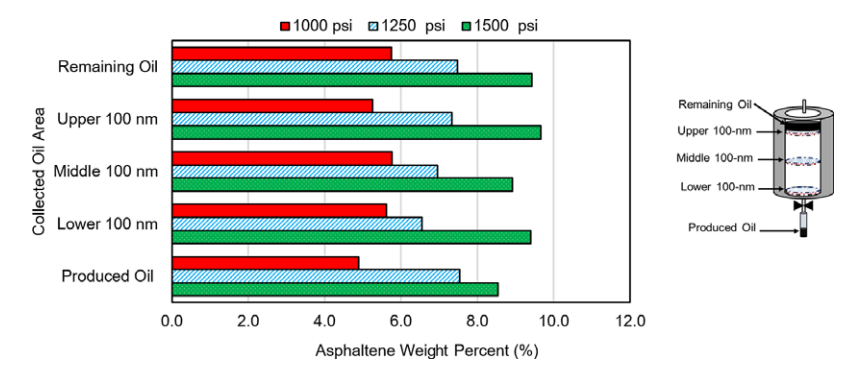


Fig. 9—Asphaltene weight percent using a uniform paper membrane distribution when injecting nitrogen at 1,000, 1,250, and 1,500 psi.

A 1,000-psi nitrogen injection pressure was selected for further investigation of the asphaltene precipitation over time. The remaining oil was collected after each experiment and dissolved in *n*-heptane at a ratio of 1:40. Various times were selected (i.e., 1, 4, and 12 hours) to investigate and visualize the asphaltene deposition process. **Fig. 10** presents the uniform asphaltene visualization tests at 1,000 psi with 100-nm pore size membranes at 32°C. The results showed an almost equal deposition process in all 100-nm membranes. At zero elapsed time, no asphaltene was observed, and the crude oil sample was entirely dissolved in *n*-heptane. After 1 hour, the asphaltene started to precipitate and form deposits such that asphaltene particles accumulated at the bottom of the tube. Over time, the solution color lightened at the top of the laboratory tubes with the presence of some suspended asphaltene particles. Finally, after 12 hours, almost all asphaltene particles were deposited, and the overall solution color was much lighter compared to the solution observed at zero time. The results confirmed that the asphaltene particles that passed through all of the filter membranes had almost the same percentage.

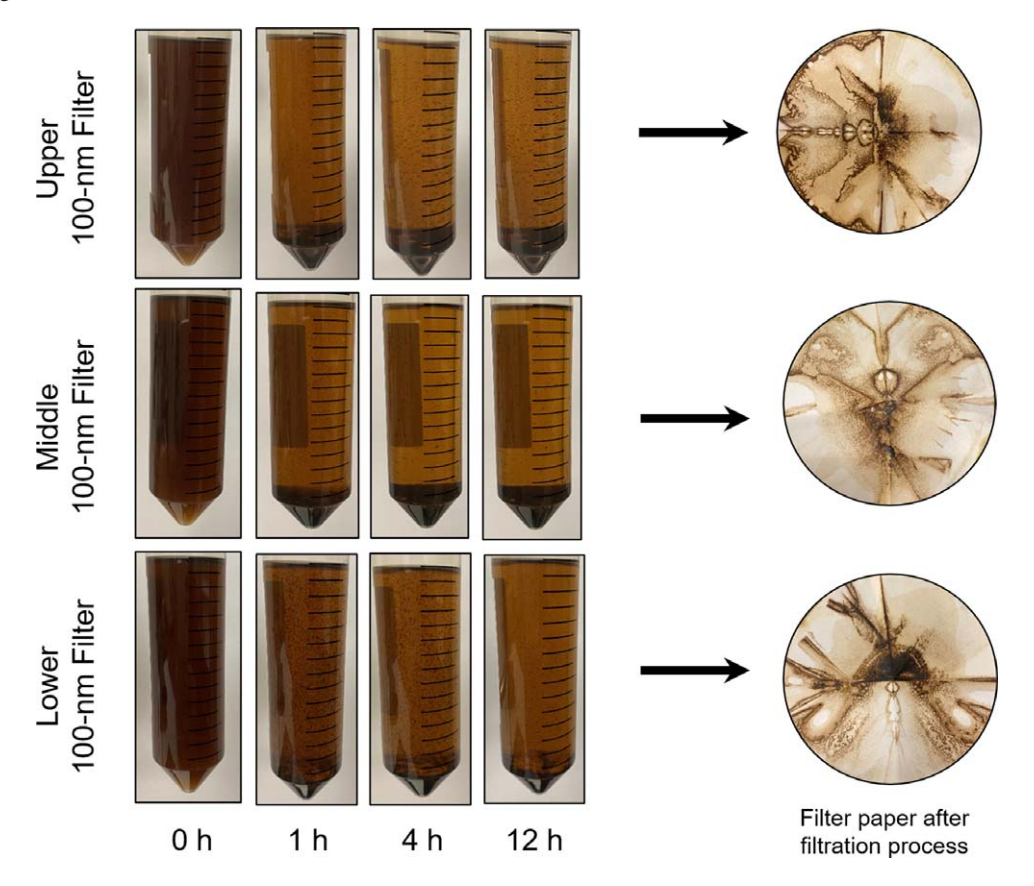


Fig. 10—Visualization of asphaltene precipitation and deposition at 1,000 psi using a uniform membrane size distribution.

Effect of Pore Size Heterogeneity. Varying the filter membrane's pore size inside the vessel created heterogeneity in the pore size distribution among membranes. Fig. 11 presents a heterogeneous paper membrane vessel consisting of (1) a filter membrane size of 450 nm located at the top of the vessel, (2) 100 nm in the middle, and (3) 50 nm at the lower part of the vessel. The experiments were conducted with nitrogen injection pressures of 1,000, 1,250, and 1,500 psi at 32°C.

Fig. 12 illustrates that as the filter membrane's pore size decreased, the asphaltene deposition increased. Furthermore, the asphaltene weight percent increased for all injection pressures. The asphaltene weight percent increased from 2.50% in 450-nm paper to 8.14% in 50-nm paper at 1,000 psi. Higher asphaltene weight percents were observed using 1,250 psi, where the percentages were 3.16 and 9.8% in 450- and 50-nm papers, respectively. Approximately 11% asphaltene weight percent was observed in a 50-nm paper membrane using 1,500 psi. These data indicate that larger pore sizes allowed the asphaltene particles to pass through and resulted in less asphaltene

precipitation. However, as the pore size of the filter membrane decreased, asphaltene particle passage was disrupted, leading to more asphaltene deposition. For instance, the asphaltene particles with a size larger than 450 nm were incapable of passing through the 450-nm filter membrane. The asphaltene particle sizes that were more than 50 nm and less than 100 nm precipitated on the 50-nm filter membrane. Asphaltene particles that were less than 50 nm could pass through the membrane and collect in the produced oil. Thus, the asphaltene that precipitated on the 450-, 100-, and 50-nm filter membranes was greater than 450 nm, between 450 and 100 nm, and between 100 and 50 nm, respectively. As a result of Brownian motion, the asphaltene aggregates continued to interact with one another, forming larger particles. Because of the large radial diffusivity of the particles, smaller aggregates have a higher tendency to deposit. In all experiments, the asphaltene weight percent in the produced oil was the lowest, because the asphaltene particles precipitated and plugged the nanopaper membranes gradually, which then led to reduced amounts of asphaltene in the oil outlet. Because of asphaltene deposition, the plugging pore size appears to be critical when increasing the nitrogen injection pressure. This could result in pore plugging and cause severe problems during production operations, thus decreasing oil recovery.

Heterogeneous Paper Membranes

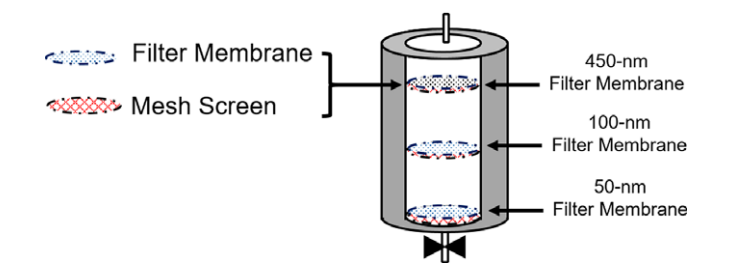


Fig. 11—Illustration of the heterogeneous paper membrane distributions inside the vessel.

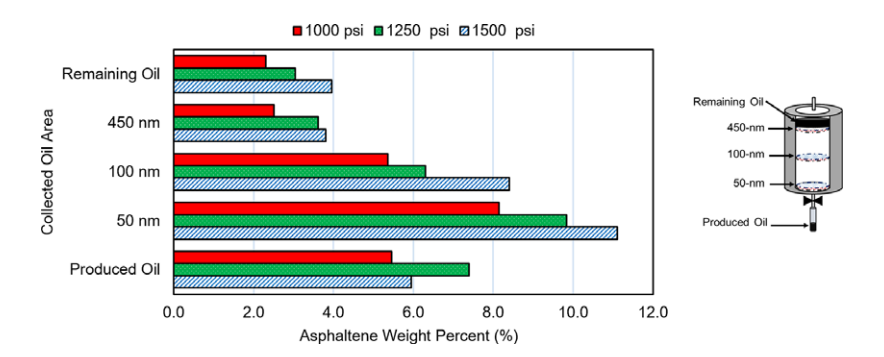


Fig. 12—Asphaltene weight percent using a heterogenous paper membrane distribution at various nitrogen injection pressures.

A 1,000-psi nitrogen injection pressure was also selected for further investigation of the asphaltene precipitation over time (Fig. 13) in a heterogeneous membrane pore size distribution. Initially, no clear asphaltene could be observed. At zero elapsed time, the solution was dark-colored for all the filter membranes. For the 450-nm filter membrane, some asphaltene deposition was seen after 1 hour, and a lighter solution color was reached after 12 hours. This could be due to the large pore size of 450 nm allowing less asphaltene particle precipitation in the filter membrane. For the 100-nm filter membrane, asphaltene deposition was observed after 1 hour and was very similar to that of the 450-nm condition. Although the observation was almost the same at this time, the final observation of the 50-nm filter after 12 hours was higher in asphaltene deposition compared to the 100- and 450-nm membranes. This indicates that smaller membrane pore sizes prevented the passage of all asphaltene particles through the membrane. It is plausible that as the filter membrane pore size decreases, some asphaltene particles cannot flow through. This is likely due to asphaltene particle sizes, which were the same or larger than the filter membrane pore size. This can be observed clearly in the 50-nm filter membrane, where after 1 hour, a darker color was observed compared to the 450- and 100-nm filters. As time progressed, some asphaltene particles were suspended in the n-heptane, and most of the asphaltene was deposited after 4 hours. Finally, greater asphaltene deposition was observed at the bottom of the test tube, signifying an elevated asphaltene deposition. In Fig. 10, the asphaltene deposition and precipitation process was similar compared to the process in the uniform tests shown in Fig. 13. In heterogenous tests, the asphaltene weight percent using the 100-nm filter membrane was 5.36% compared to 5.26% in the upper part of the 100-nm filter membrane in the uniform test. This confirms that the same pore size will be impacted by asphaltene clusters in the same way under the same conditions, as it is here with the same pressure of 1,000 psi.

Further visualization analysis of asphaltene was obtained at 1,000, 1,250, and 1,500 psi using asphaltene collected from the remaining oil. Fig. 14 shows the asphaltene visualization experiments with different pressures at 32°C with a 2-hour mixing time. With 0 hours elapsed, all of the tubes showed almost the same results at all pressures: Asphaltene was entirely dissolved in *n*-heptane, and no clear asphaltene depositions or precipitations were observed. After 1 hour, the asphaltene started to flocculate in the tubes, especially at 1,250 and 1,500 psi, as displayed in the representative images. Interestingly, for 1,000 psi, no clear asphaltene deposition was observed, and the particles appeared to remain stable because of exposure to a lower nitrogen injection pressure. After 4 hours, the flocculation had begun to settle, and deposits were observed at the bottom of the tube, with more deposits at the highest pressure (i.e., 1,500 psi). This indicates that higher pressure affected the instability of asphaltene faster than did the lower pressure. As time progressed, more asphaltene deposition was observed under all conditions. The lighter the color of the mixture, the higher the asphaltene deposition at the bottom of the tubes. The visualization experiments showed that the asphaltene flocculation requires time to complete, making time a crucial factor in the asphaltene precipitation process. Detecting and understanding asphaltene deposition over time can facilitate mitigating the expected formation damage.

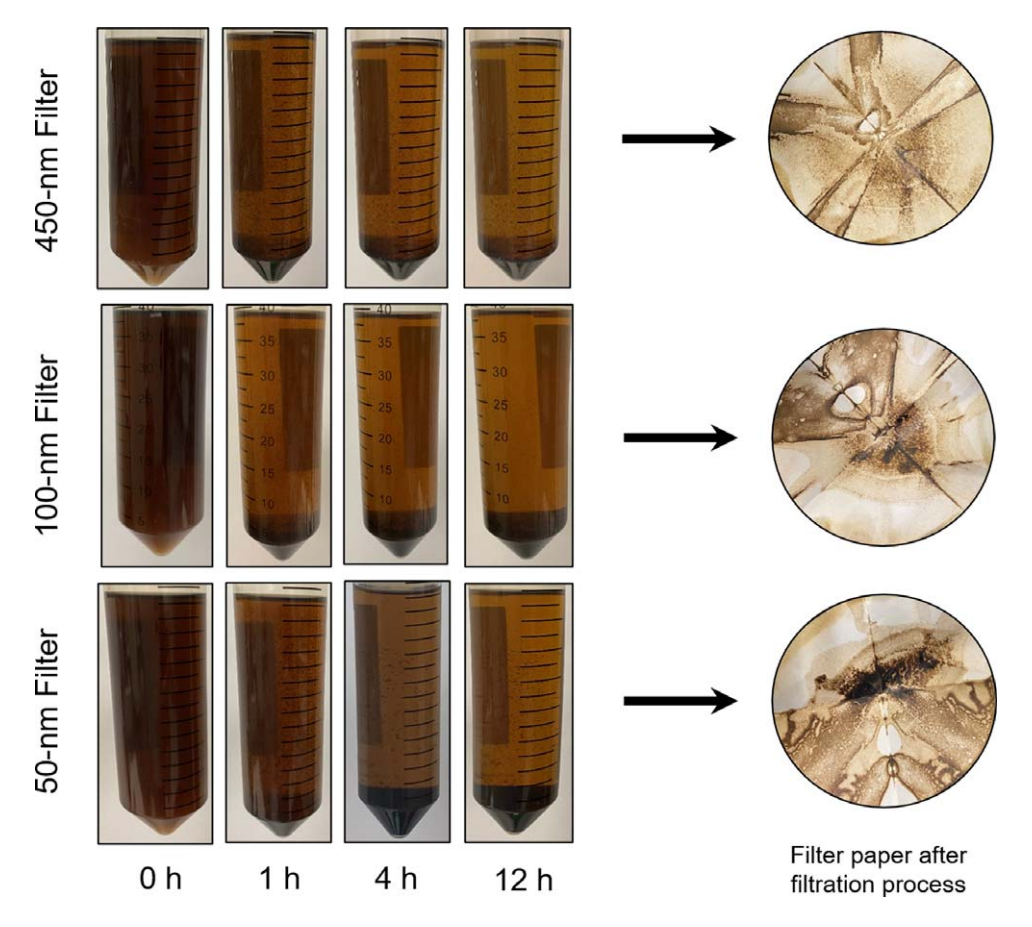


Fig. 13—Visualization of asphaltene precipitation and deposition at 1,000 psi using a heterogeneous distribution.

Effect of Mixing Time. Mixing time is defined as the total time the oil was exposed to the desired nitrogen pressure inside the filtration cell and left at 32°C to let the nitrogen mix well with the crude oil. Times of 10, 60, and 120 minutes were selected to investigate the effect of the mixing time on the asphaltene precipitation and deposition during 1,000 psi nitrogen injection at a temperature of 32°C. Fig. 15 highlights that increasing the mixing time resulted in a slight increase in the asphaltene weight percent. For 450-nm paper, the asphaltene weight percent ranged from 3.7 to 5.17% for the mixing times of 10 minutes and 2 hours, respectively. It was observed that decreasing the filter membrane size led to an increase in asphaltene weight percent. This is due to the pore plugging from asphaltene clusters. For the 50-nm paper membrane, there were notable increases in the asphaltene weight percent, especially for 60-and 120-minute mixing times. However, there were no significant differences between the asphaltene weight percentages in each filter membrane for these two mixing times. These data indicate that the mixing time did not have an intrinsic effect on the asphaltene deposition within 120 minutes but might cause a slight effect over longer times. Increased mixing times that expose the crude oil to nitrogen will increase the asphaltene weight percent, thus increasing the precipitation and deposition of asphaltene, especially in smaller pores.

Fig. 16 shows the asphaltene precipitation process of nitrogen injections at 1,000 psi for 10-, 60-, and 120-minute mixing times at 32°C. As mentioned previously, the results of the visualization experiments indicated that increased mixing time also increased the asphaltene deposition and precipitation process. For a 10-minute mixing time, the asphaltene deposition process was relatively slow, and the asphaltene settled after 12 hours. The solution at the top of the tube after 1 hour was still dark brown in color, which suggests less settling at this time interval. However, after 120 minutes of mixing time, the bottommost section of the tube was dark after 1 hour of settling, whereas a lighter color was observed at the top of the tube. The asphaltene continued to settle, and sediment at the bottom of the tube was substantially darker after 4 hours. After 12 hours of settling, there were no significant observable changes in the asphaltene deposition process for all initial mixing times. Given these observations, it is necessary to analyze asphaltene instability and the effect of the mixing time to avoid any asphaltene-related problems. After the filtration process, the filter membranes exhibited a higher asphaltene percent after 120 minutes of mixing time compared to 10 minutes.

Effect of Temperature on Asphaltene Deposition. All of the previously described experiments were conducted at 32°C, but the effect of a higher temperature will be discussed in this section. Temperature can strongly impact asphaltene deposition and precipitation in crude oil. Two experiments were conducted at two temperatures (i.e., 32 and 70°C) to investigate the effect of a high temperature on the asphaltene stability. The 32°C represents room temperature, and 70°C represents the average temperature of shale basins. In both experiments, the entire filtration vessel was placed inside an oven to ensure the stability of the required temperature. A pressure of 1,000 psi for the nitrogen injection and a 2-hour mixing time were used in both experiments. Fig. 17 shows that increasing the temperature resulted in a decrease in the asphaltene weight percent. The higher asphaltene weight percent was observed in the 50-nm filter membrane: 5.11 and 3.12% for 32 and 70°C, respectively. This is likely due to the bonds between asphaltene and resins in the crude oil structure being weakened by the increased temperature, which increased the rate of asphaltene precipitation. The higher the temperature, the higher the asphaltene solubility rate and the lower the asphaltene concentrations. In stable oils, the suspension colloidal particles of asphaltene are covered by resins that are strongly connected to the asphaltene. This connection between asphaltene and resins becomes stronger at higher temperatures, which keeps the asphaltene dissolved in oil (Hoepfner et al. 2013). At higher temperatures, a smaller amount of asphaltene colloidal will form, and it will tend not to create strong associations because of the colloids being dispersed effectively by the resins (Branco et al. 2001). The precipitated asphaltenes that develop from the colloidal suspension particles

at higher temperatures tend to dissolve in the oil; thus, more asphaltenes will form in soluble conditions but fewer in colloidal conditions (Chandio et al. 2015). The resins can have a tendency to self-associate, and that tendency is much stronger at lower temperatures. Therefore, the bond between asphaltene and resins weaken (Pereira et al. 2007). Consequently, greater asphaltene precipitation can form because of the molecules of asphaltene becoming stronger in terms of their polarity, resulting in more aggregation at lower temperatures. Also, membrane pore size had the same effect at both temperatures: as the filter paper membrane pore size decreased, the asphaltene weight percent increased. This is because the asphaltene particle size plugged the pores much more in the 50-nm filter membrane; thus, more asphaltene was observed.

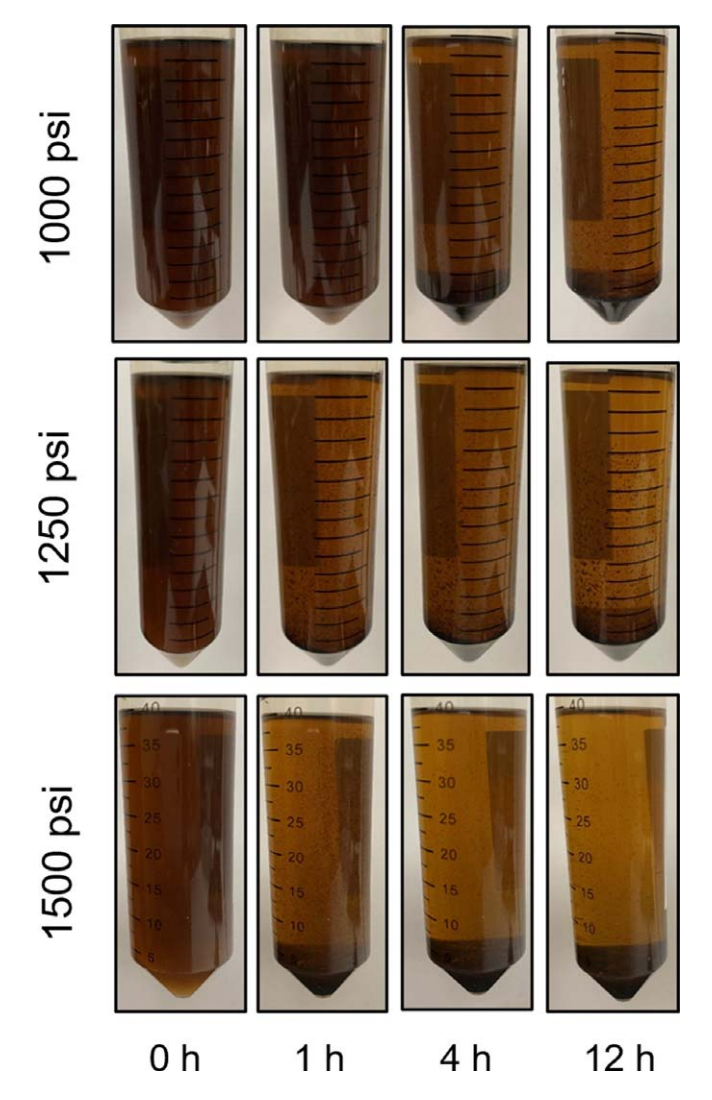


Fig. 14—Asphaltene precipitation and deposition visualization of the remaining oil using different pressures at 32°C with a 2-hour mixing time.

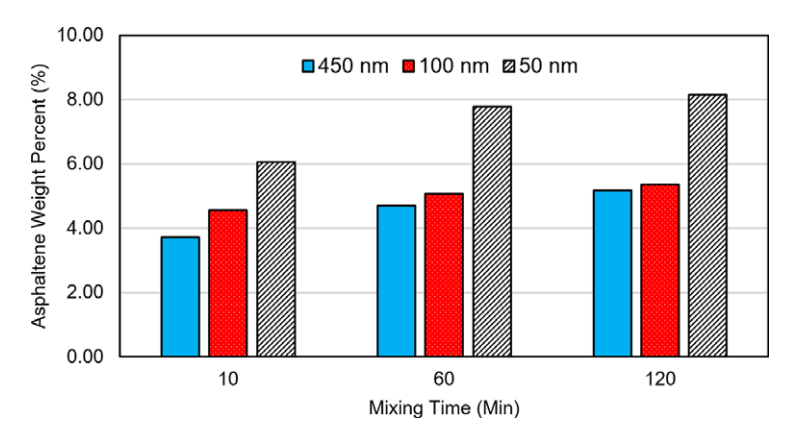


Fig. 15—Asphaltene weight percent at 10, 60, and 120 minutes of mixing time using 450-, 100-, and 50-nm filter membranes.

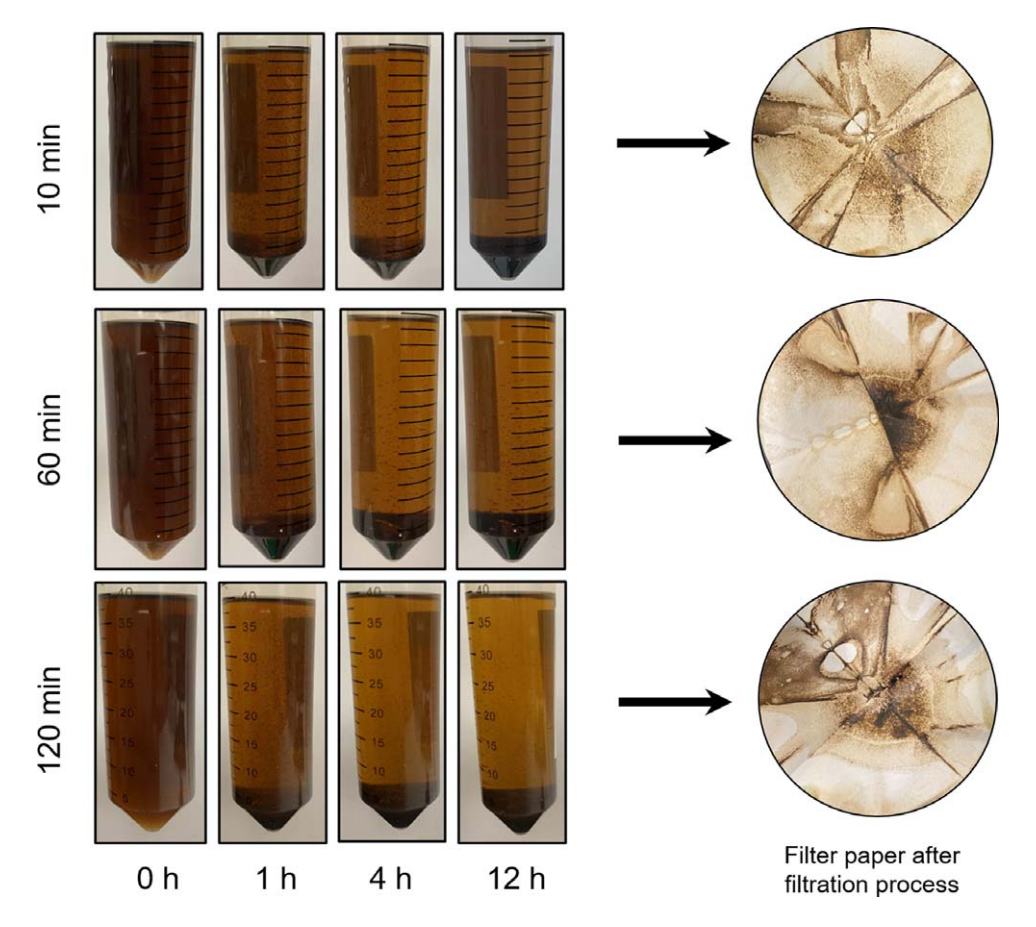


Fig. 16—Visualization of asphaltene precipitation and deposition at different mixing times.

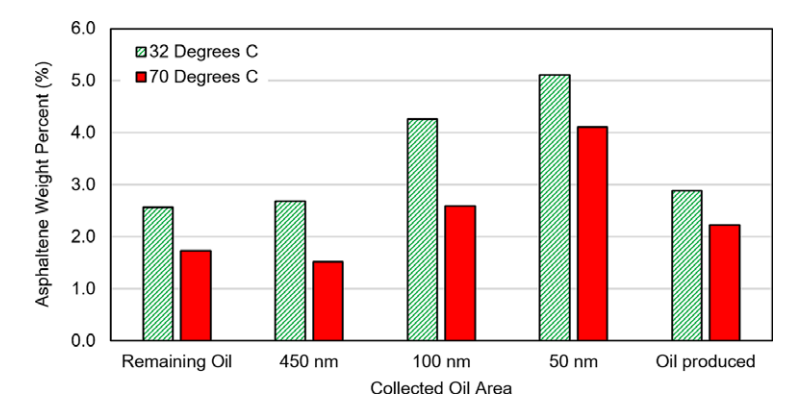


Fig. 17—Asphaltene weight percent at different temperatures using 1,000 psi.

Further Analysis and Discussion

Chromatography Analysis. Gas chromatography-mass spectrometry (GC6890-MS5973) was used to detect the main chemical components and their presence in the produced oil, including asphaltene, to confirm the results mentioned previously concerning asphaltene aggregation. Table 3 presents the gas chromatography analysis before and after the nitrogen gas injection experiments at 1,000 and 1,500 psi. First, the original crude oil with 19 cp was analyzed to compare its components to the oil after the experiments. The oil produced from the nitrogen injection pressures at 1,000 and 1,500 psi was selected to highlight the asphaltene changes. The asphaltene components are included in the heavy components of C_{30+} . The analysis showed that when increasing the pressure, the heavy components also increased. The heavy compounds, including asphaltene, decreased from 5.17 to 1.96% with a 1,000 psi gas injection, which confirmed that the filter membranes inside the filtration vessel had a significant effect on the heavy components, including the asphaltene. The asphaltene molecules plugged the filter membrane's pores gradually, thus reducing the asphaltene content at the outlet that produced the oil. However, the analysis showed that a higher pressure of 1,500 psi produced fewer asphaltene components (2.50%) compared to the original oil (5.17%) but higher than the compounds compared to 1,000 psi (i.e., 1.96%). This results from the higher injection pressure causing the resins around the asphaltene molecules to weaken, thus providing a higher asphaltene content.

Weight Percent (%)

	Before Experiment	After Experiment		
Components	(original oil)	1,000 psi	1,500 psi	
C ₈ to C ₁₄	65.14	87.43	92.43	
C ₁₅ to C ₁₉	6.06	3.59	2.20	
C ₂₀ to C ₂₄	9.16	2.27	1.25	
C ₂₅ to C ₂₉	14.48	4.76	1.62	
C ₃₀ + (including asphaltene)	5.17	1.96	2.50	
Total	100.00	100.00	100.00	

Table 3—Gas chromatography analysis before and after the experiments with 1,000 and 1,500 psi nitrogen gas injection.

Microscopy Imaging Analysis. The asphaltene particles were induced by gas injection, where large asphaltene clusters can form, leading to asphaltene holdup in a reservoir. Asphaltene can plug the pores and cause severe problems, including a reduction in oil relative permeability, alteration of the wettability of the rock, and an overall reduction in oil production. The filter paper membranes of 450 and 50 nm with 1,500 psi gas injection were cleaned by the solvent *n*-heptane to highlight the pore plugging in the filter paper. **Fig. 18** illustrates the filter membrane before and after conducting the filtration experiment as well as after cleaning the crude oil from the filter membrane. The photo shows the asphaltene deposited in the filter membrane pores and the plugged path through which the crude oil had to move, especially in the 50-nm filter membrane, because of its smaller pore size.

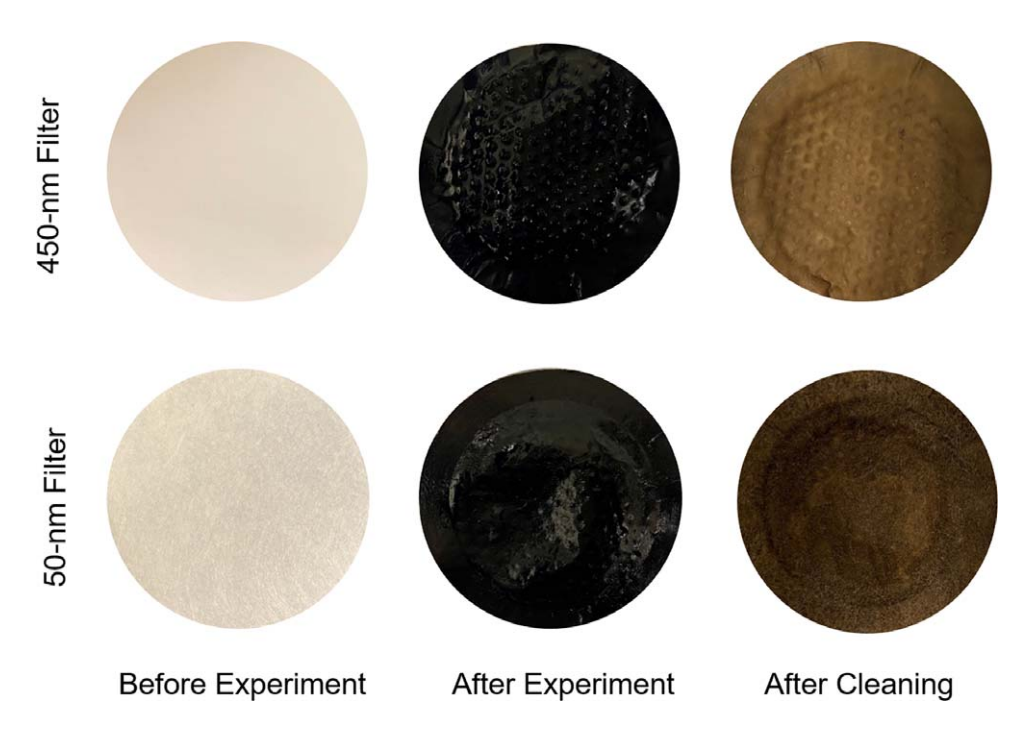


Fig. 18—Illustration of the filter membranes (450- and 50-nm) at 1,500 psi before and after the experiment and after cleaning.

For a better understanding of the effect of asphaltene on pore plugging, a digital microscope was used to identify the plugging pores in the filter membranes. Showing the filter membranes' microstructure will highlight the severity of the asphaltene aggregation on different pore size structures. **Fig. 19** displays the microscopic images (20 µm) of the filter membrane's pore structure of 450-, 100-, and 50-nm filters using a nitrogen injection pressure of 1,000, 1,250, and 1,500 psi at 32°C. The images were captured after cleaning and exposing the filter membranes to an *n*-heptane solvent for 24 hours. Obvious differences occurred in the aggregation of the precipitated asphaltene molecules in the filter membrane images: The higher pressure coupled with a filter membrane having a smaller pore size resulted in more deposition of asphaltene and increased amounts of pore plugging, which is evident in the darker color of the images.

SEM Analysis. SEM is an advanced imaging analysis that can determine pore structure, particularly in unconventional shale structures that are known for their small pore sizes. SEM was used to highlight the impact of pressure and asphaltene particles on pore size plugging. To illustrate this, a collection of SEM images was taken for all heterogenous filter membranes (i.e., 450-, 100-, and 50-nm) during nitrogen injection at 1,000 and 1,500 psi. **Fig. 20** provides SEM images (5 μm) of the filter membranes' pore structure of the 450-, 100-, and 50-nm filter paper using an nitrogen injection pressure of 1,000 and 1,500 psi at 32°C. For the 450-nm filter paper, the images depict asphaltenes accumulated inside the structure, which were black in color at injection pressures of 1,000 and 1,500 psi. The filter

paper pore plugging was more severe in the 450-nm filter membrane using 1,500 psi. The structure of the of 450-nm filter membranes was captured clearly because of the larger pore size compared to the 100- and 50-nm filters. As the pore size of the filter membrane decreased, dark colors were observed for the 100-nm filter membrane. Most of the area of the 100-nm filter papers was affected by asphaltene depositions, with the darkest color occurring at an injection pressure of 1,500 psi. This confirms that the asphaltenes had more impact on the smallest pore structure compared to the largest (450 nm). Because of their smaller pore sizes, most of the photo areas of the 50-nm filter membranes were obstructed by asphaltenes.

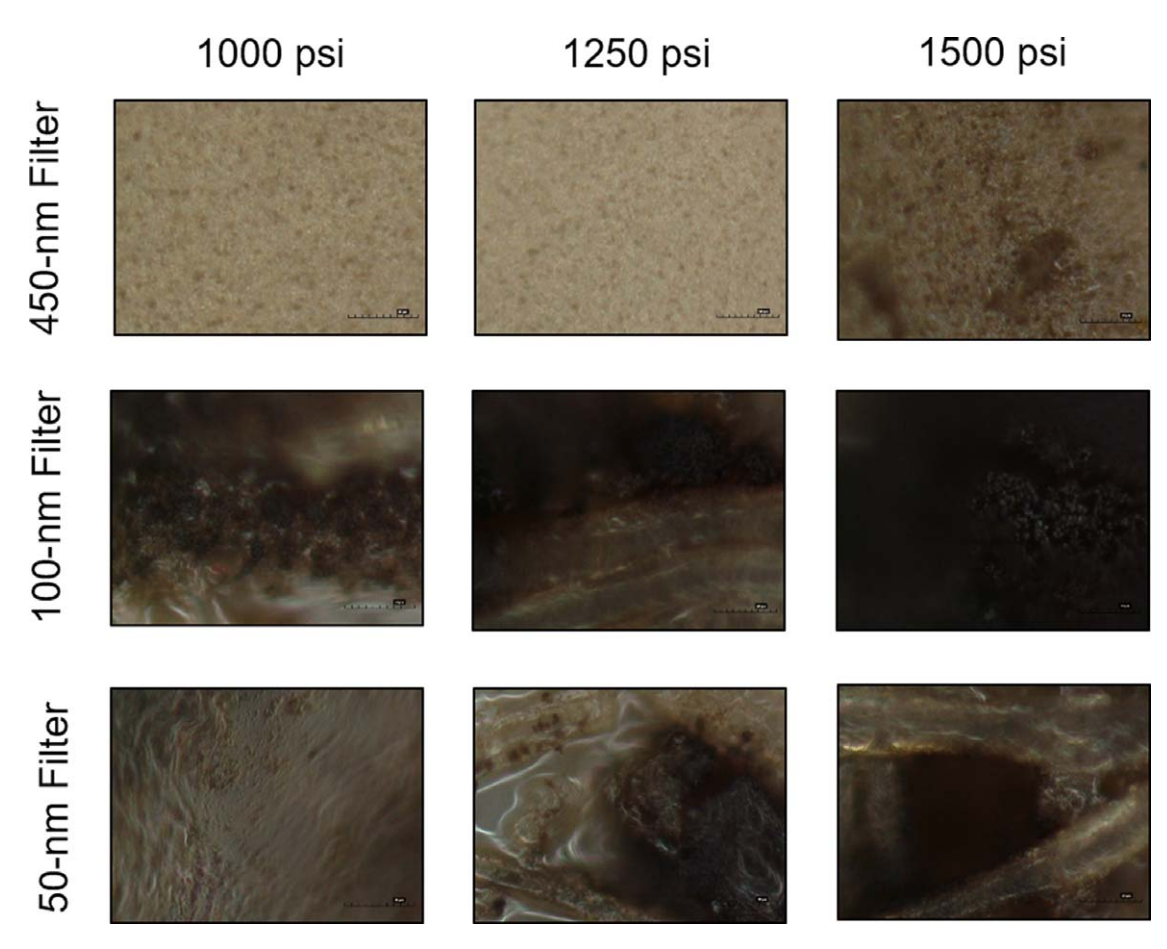


Fig. 19—Digital microscopic images (20 μm) of 450-, 100-, and 50-nm filter membranes using various nitrogen injection pressures.

Pore Size Reduction Caused by Asphaltene Deposition. To identify the effect of asphaltene on the pore plugging of the filter paper membranes, SEM images were processed using computer software to analyze the pore size of each filter membrane. Fig. 21 compares the pore size distribution in the 450-nm filter membrane after nitrogen injections at 1,000 and 1,500 psi. The estimated pore size distribution of the 450-nm filter paper ranged from 40 to 400 nm at 1,000 psi and from 50 nm to 200 nm at 1,500 psi. The results showed that higher pressure (1,500 psi) had a greater impact on pore plugging compared to the lower pressure (1,000 psi) because the higher pressure created more asphaltene particles and resulted in higher asphaltene precipitation and deposition, which reduced the pore sizes. The oil path in the filter membranes became smaller because of the asphaltene deposition. The same observations were found in 100- and 50-nm filter membranes. For the 100-nm filter membrane, the pore size distribution ranged from 10 and 50 nm for the lower pressure (1,000 psi) and from 15 to 35 nm for the higher pressure (1,500 psi), as shown in Fig. 22. A smaller pore size distribution was observed in the 50-nm filter membrane because of the smaller size of the pores. Fig. 23 presents the results of the pore size distribution in the 50-nm filter membrane. The asphaltene particles accumulated at higher percentages in the smaller pore sizes of the filter membranes and then plugged most of the pores. Smaller pore size leads to more asphaltene concentration, which leads to more pore plugging. Su et al. (2021) developed an integrated simulation approach to predict permeability reduction under asphaltene particle aggregation and deposition. They concluded that longer aggregation time, higher flow velocity, and bigger precipitation concentrations will lead to a faster reduction in permeability. Thus, these results from this study revealed that asphaltenes in crude oil can be induced by nitrogen injection and cause severe issues in pore plugging, especially in unconventional resources with a small pore size.

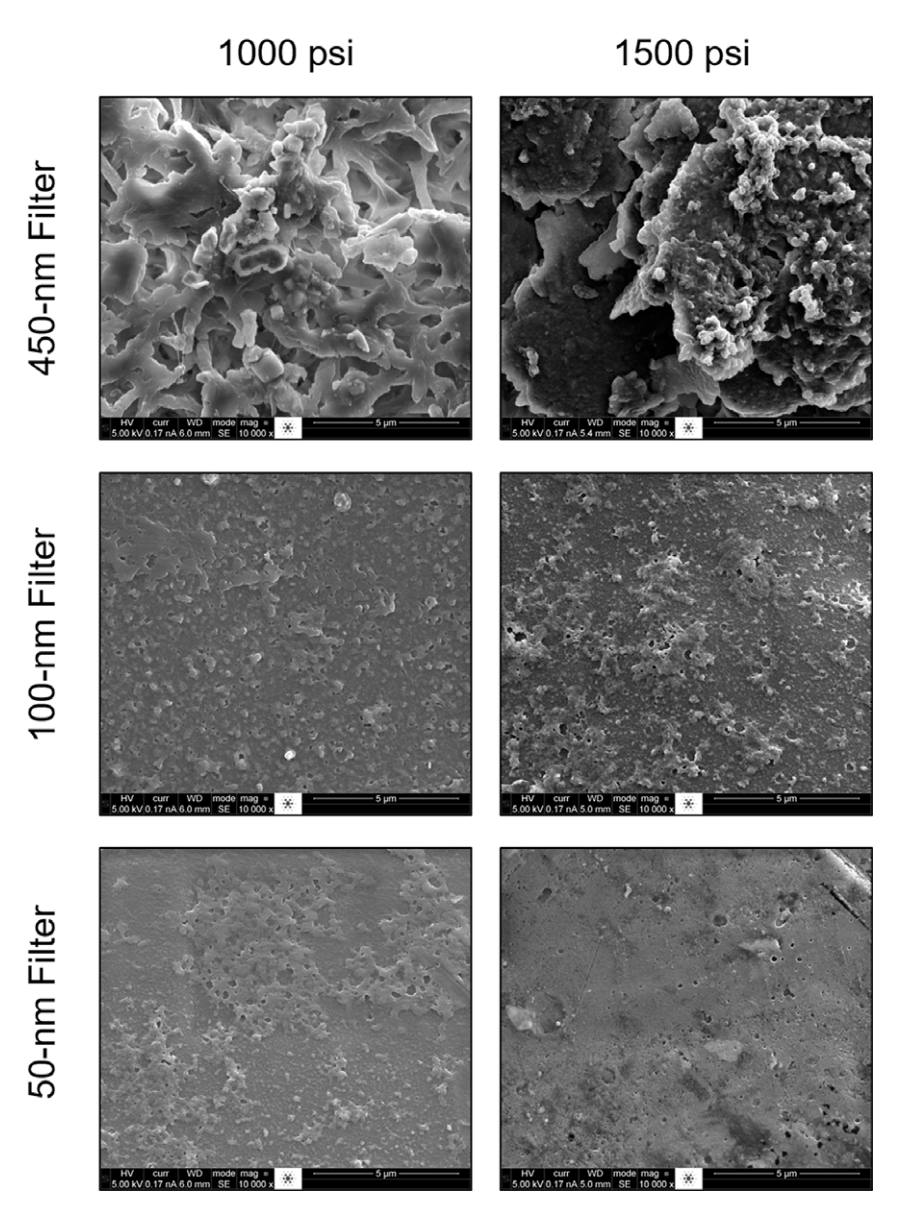


Fig. 20—SEM images (5 µm) of 450-, 100-, and 50-nm filter membranes at 1,000 and 1,500 psi injection pressure.

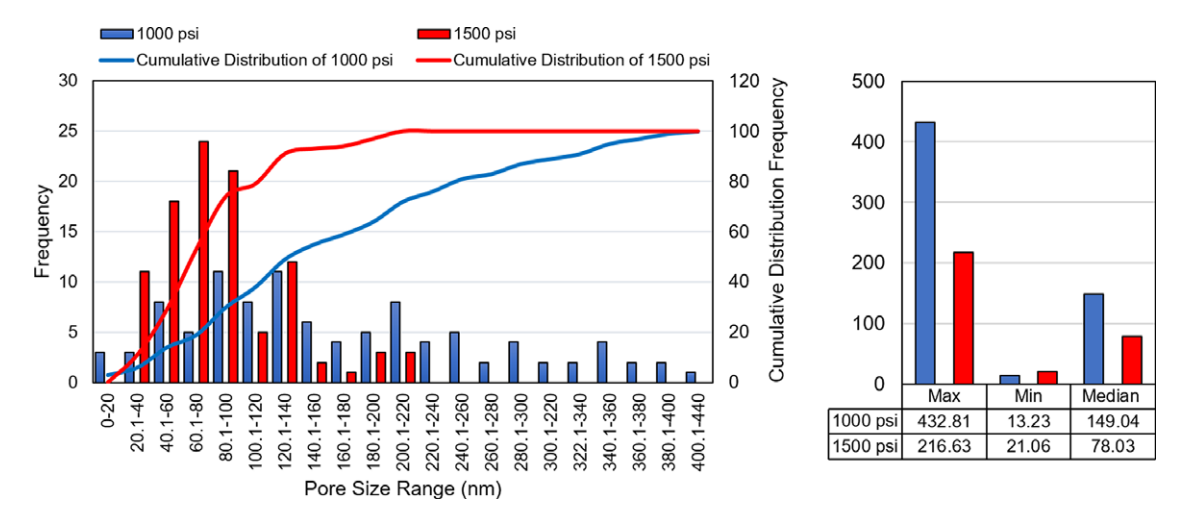


Fig. 21—Comparison of the pore size distribution in a 450-nm filter membrane after 1,000- and 1,500-psi nitrogen injections.

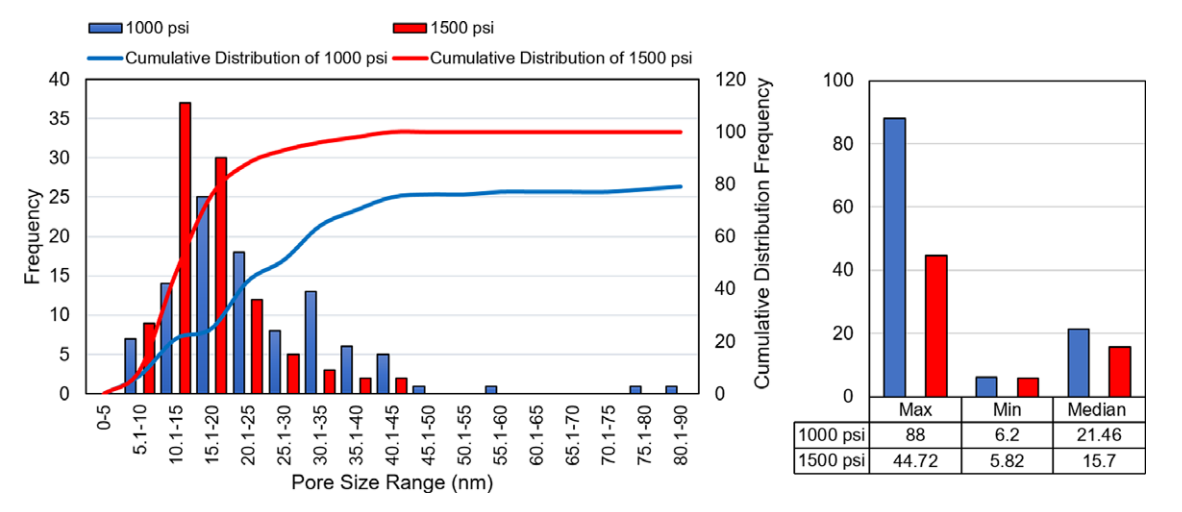


Fig. 22—Comparison of the pore size distribution in a 100-nm filter membrane after 1,000- and 1,500-psi nitrogen injections.

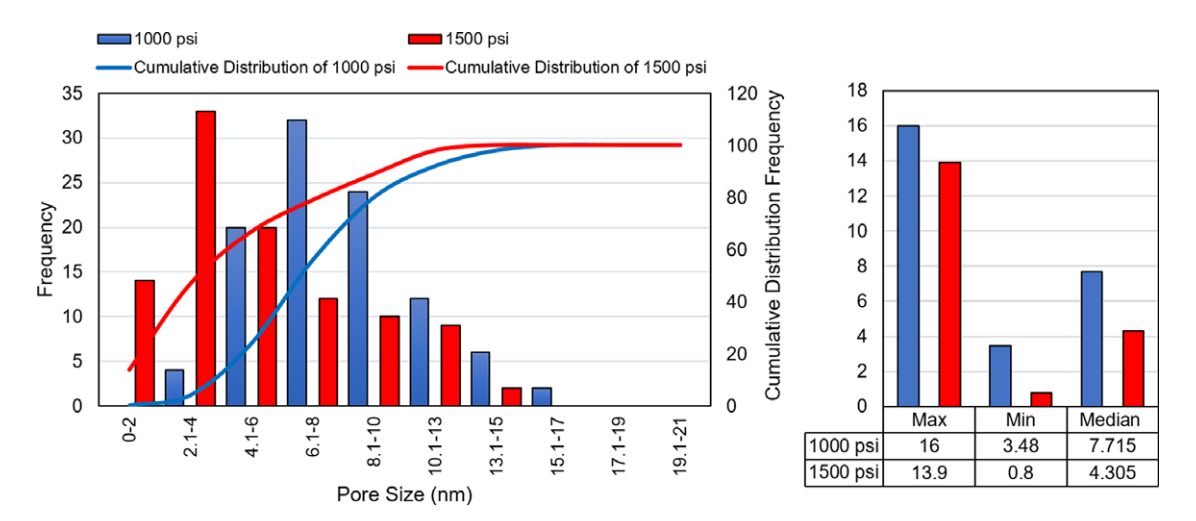


Fig. 23—Comparison of the pore size distribution in a 50-nm filter membrane after 1,000- and 1,500-psi nitrogen injections.

Conclusions

Three sets of experiments investigated nitrogen immiscible pressure, filtration, and visualization of asphaltene. The asphaltene stability in crude oil was observed and investigated during nitrogen injection. Various factors including injection pressure, temperature, mixing time, filter membrane distribution, and pore size were investigated. The results support the following conclusions:

- 1. As the nitrogen injection pressure rose, the asphaltene weight percent also rose. Increasing the injection pressure resulted in a slight increase in the asphaltene deposition time.
- 2. As the pore size decreased in the heterogeneous pore size distribution, asphaltene clusters were unable to pass through easily. Subsequently, asphaltene precipitation and deposition increased.
- 3. Using a uniform pore size distribution inside a vessel with a 100-nm filter gave almost the same asphaltene weight percent for all of the filter paper membranes because the same asphaltene particles passed through all of the same pore-sized membranes.
- 4. Increasing the temperature resulted in a decrease in the asphaltene weight percent. The higher the temperature, the higher the asphaltene solubility rate, and the lower the asphaltene concentrations.
- 5. The results demonstrated that increasing the mixing time, which exposed the crude oil to the nitrogen for a longer time, increased the asphaltene instability, leading to increases in asphaltene precipitation and deposition.
- The chromatography results demonstrated that the weight percent of the heavy components, including asphaltene, was higher when using 1,500 psi than when using 1,000 psi.
- 7. The microscopy imaging demonstrated the severity of the asphaltene deposition on the pore plugging. The results showed an increase in pore plugging when the pressure rose combined with a decrease in the pore size of the filter membranes.
- 8. SEM observation confirmed that at a higher pressure and with a smaller pore size, the asphaltene particles created more severe pore plugging. Pore size distribution analysis indicated that the pore size decreased significantly in all filter paper membranes because of asphaltene plugging.

Acknowledgments

The authors acknowledge the National Science Foundation, Chemical, Biological, Environmental, and Transport systems for funding the work under Grant CBET-1932965.

References

- Alta'ee, A. F., Hun, O. S., Alian, S. S. et al. 2012. Experimental Investigation on the Effect of CO₂ and WAG Injection on Permeability Reduction Induced by Asphaltene Precipitation in Light Oil. *Int J Mater Metall Eng* **6** (12): 1203–1208. https://doi.org/10.5281/zenodo.1078765.
- Belhaj, H., Abu Khalifeh, H. A., and Javid, K. 2013. Potential of Nitrogen Gas Miscible Injection in South East Assets, Abu Dhabi. Paper presented at the North Africa Technical Conference and Exhibition, Cairo, Egypt, 15–17 April. SPE-164774-MS. https://doi.org/10.2118/164774-MS.
- Branco, V. A. M., Mansoori, G. A., Xavier, L. C. D. A. et al. 2001. Asphaltene Flocculation and Collapse from Petroleum Fluids. *J Pet Sci Eng* 32 (2–4): 217–230. https://doi.org/10.1016/S0920-4105(01)00163-2.
- Buriro, M. A. and Shuker, M. T. 2012. Asphaltene Prediction and Prevention: A Strategy To Control Asphaltene Precipitation. Paper presented at the SPE/PAPG Annual Technical Conference, Islamabad, Pakistan, 3–5 December. SPE-163129-MS. https://doi.org/10.2118/163129-MS.
- Buriro, M. and Shuker, M. T. 2013. Minimizing Asphaltene Precipitation in Malaysian Reservoir. Paper presented at the SPE Saudi Arabia Section Technical Symposium and Exhibition, Al-Khobar, Saudi Arabia, 19–22 May. SPE-168105-MS. https://doi.org/10.2118/168105-MS.
- Chandio, Z. A., Ramasamy, M., and Mukhtar, H. B. 2015. Temperature Effects on Solubility of Asphaltenes in Crude Oils. *Chem Eng Res Des* 94: 573–583. https://doi.org/10.1016/j.cherd.2014.09.018.
- Chung, T. H. 1992. Thermodynamic Modeling for Organic Solid Precipitation. Paper presented at the SPE Annual Technical Conference and Exhibition, Washington, D.C., USA, 4–7 October. SPE-24851-MS. https://doi.org/10.2118/24851-MS.
- Dahaghi, A. K., Gholami, V., Moghadasi, J. et al. 2008. Formation Damage through Asphaltene Precipitation Resulting from CO₂ Gas Injection Iranian Carbonate Reservoir. SPE Prod & Oper 23 (2): 210–214. SPE-99631-PA. https://doi.org/10.2118/99631-PA.
- Elturki, M. and Imqam, A. 2020a. High Pressure-High Temperature Nitrogen Interaction with Crude Oil and Its Impact on Asphaltene Deposition in Nano Shale Pore Structure: An Experimental Study. Paper presented at the SPE/AAPG/SEG Unconventional Resources Technology Conference, Virtual, 20–22 July. URTEC-2020-3241-MS. https://doi.org/10.15530/urtec-2020-3241.
- Elturki, M. and Imqam, A. 2020b. Application of Enhanced Oil Recovery Methods in Unconventional Reservoirs: A Review and Data Analysis. Alexandria, Virginia, USA: American Rock Mechanics Association.
- Elturki, M. and Imqam, M. 2021. Analysis of Nitrogen Minimum Miscibility Pressure (MMP) and Its Impact on Instability of Asphaltene Aggregates: An Experimental Study. Paper presented at the SPE Trinidad and Tobago Section Energy Resources Conference Virtual, 28–30 June. SPE-200900-MS. https://doi.org/10.2118/200900-MS.
- Elwegaa, K. and Emadi, H. 2019. Improving Oil Recovery from Shale Oil Reservoirs Using Cyclic Cold Nitrogen Injection: An Experimental Study. Fuel 254: 115716. https://doi.org/10.1016/j.fuel.2019.115716.
- Fakher, S., Ahdaya, M., Elturki, M. et al. 2019a. The Effect of Unconventional Oil Reservoirs' Nano Pore Size on the Stability of Asphaltene during Carbon Dioxide Injection. Paper presented at the Carbon Management Technology Conference, Houston, Texas, USA, 15–18 July. CMTC-558486-MS. https://doi.org/10.7122/CMTC-558486-MS.
- Fakher, S., Ahdaya, M., Elturki, M. et al. 2019b. Roadmap to Asphaltene Characteristics, Properties, and Presence in Crude Oils Based on an Updated Database from Laboratory Studies. Paper presented at the Carbon Management Technology Conference, Houston, Texas, USA, 13 November. CMTC-558560-MS. https://doi.org/10.7122/CMTC-558560-MS.
- Fakher, S., Ahdaya, M., Elturki, M. et al. 2020a. Critical Review of Asphaltene Properties and Factors Impacting Its Stability in Crude Oil. *J Pet Explor Prod Technol* 10 (3): 1183–1200. https://doi.org/10.1007/s13202-019-00811-5.
- Fakher, S., Ahdaya, M., Elturki, M. et al. 2020b. An Experimental Investigation of Asphaltene Stability in Heavy Crude Oil during Carbon Dioxide Injection. *J Pet Explor Prod Technol* **10** (3): 919–931. https://doi.org/10.1007/s13202-019-00782-7.
- Fakher, S. and Imqam, A. 2019. Asphaltene Precipitation and Deposition during CO₂ Injection in Nano Shale Pore Structure and Its Impact on Oil Recovery. Fuel 237: 1029–1039. https://doi.org/10.1016/j.fuel.2018.10.039.
- Gamadi, T. D., Sheng, J. J., and Soliman, M. Y. 2013. An Experimental Study of Cyclic Gas Injection To Improve Shale Oil Recovery. Paper presented at the SPE Annual Technical Conference and Exhibition, New Orleans, Louisiana, USA, 30 September–2 October. SPE-166334-MS. https://doi.org/10.2118/166334-MS.
- Goual, L. and Firoozabadi, A. 2002. Measuring Asphaltenes and Resins, and Dipole Moment in Petroleum Fluids. *AIChE J* 48 (11): 2646–2663. https://doi.org/10.1002/aic.690481124.
- Hajizadeh, A., Ravari, R. R., and Amani, M. 2009. The Comparison of Effects of Injection of Natural/Nitrogen Gases on Asphaltene Precipitation Process. Paper presented at the SPE/EAGE Reservoir Characterization and Simulation Conference, Abu Dhabi, UAE, 19–21 October. SPE-123368-MS. https://doi.org/10.2118/123368-MS.
- Hassanpouryouzband, A., Joonaki, E., Taghikhani, V. et al. 2018. New Two-Dimensional Particle-Scale Model To Simulate Asphaltene Deposition in Wellbores and Pipelines. *Energy Fuels* 32 (3): 2661–2672. https://doi.org/10.1021/acs.energyfuels.7b02714.
- Hassanpouryouzband, A., Yang, J., Tohidi, B. et al. 2019. Geological CO₂ Capture and Storage with Flue Gas Hydrate Formation in Frozen and Unfrozen Sediments: Method Development, Real Time-Scale Kinetic Characteristics, Efficiency, and Clathrate Structural Transition. ACS Sustain Chem Eng 7 (5): 5338–5345. https://doi.org/10.1021/acssuschemeng.8b06374.
- Hoepfner, M. P., Limsakoune, V., Chuenmeechao, V. et al. 2013. A Fundamental Study of Asphaltene Deposition. *Energy Fuels* 27 (2): 725–735. https://doi.org/10.1021/ef3017392.
- Jamaluddin, A. K. M., Joshi, N., Iwere, F. et al. 2002. An Investigation of Asphaltene Instability under Nitrogen Injection. Paper presented at the SPE International Petroleum Conference and Exhibition in Mexico, Villahermosa, Mexico, 10–12 February. SPE-74393-MS. https://doi.org/10.2118/74393-MS.
- Khalaf, M. H. and Mansoori, G. A. 2019. Asphaltenes Aggregation during Petroleum Reservoir Air and Nitrogen Flooding. *J Pet Sci Eng* 173: 1121–1129. https://doi.org/10.1016/j.petrol.2018.10.037.
- Mansoori, G. A. and Elmi, A. 2010. Remediation of Asphaltene and Other Heavy Organic Deposits in Oil Wells and in Pipelines. *Socar Proc* **4:** 12–23. https://doi.org/10.5510/OGP20100400039.
- Maroudas, A. 1966. Particles Deposition in Granular Filter Media-2. Filtrat Sep 3 (2): 115–121.
- Moradi, S., Dabiri, M., Dabir, B. et al. 2012b. Investigation of Asphaltene Precipitation in Miscible Gas Injection Processes: Experimental Study and Modeling. *Braz J Chem Eng* **29** (3): 665–676. https://doi.org/10.1590/S0104-66322012000300022.
- Moradi, S., Dabir, B., Rashtchian, D. et al. 2012a. Effect of Miscible Nitrogen Injection on Instability, Particle Size Distribution, and Fractal Structure of Asphaltene Aggregates. *J Dispers Sci Technol* 33 (5): 763–770. https://doi.org/10.1080/01932691.2011.567878.
- Mozaffari, S., Tchoukov, P., Atias, J. et al. 2015. Effect of Asphaltene Aggregation on Rheological Properties of Diluted Athabasca Bitumen. *Energy Fuels* 29 (9): 5595–5599. https://doi.org/10.1021/acs.energyfuels.5b00918.
- Necmettin, M. 2003. High Pressure Nitrogen Injection for Miscible/Immiscible Enhanced Oil Recovery. Paper presented at the SPE Latin American and Caribbean Petroleum Engineering Conference, Port-of-Spain, Trinidad and Tobago, 27–30 April. SPE-81008-MS. https://doi.org/10.2118/81008-MS.

- Nguyen, M. T., Nguyen, D. L. T., Xia, C. et al. 2020. Recent Advances in Asphaltene Transformation in Heavy Oil Hydroprocessing: Progress, Challenges, and Future Perspectives. Fuel Process Technol 106681. https://doi.org/10.1016/j.fuproc.2020.106681.
- Pereira, J. C., López, I., Salas, R. et al. 2007. Resins: The Molecules Responsible for the Stability/Instability Phenomena of Asphaltenes. *Energy Fuels* 21 (3): 1317–1321. https://doi.org/10.1021/ef0603333.
- Ren, B., Xu, Y., Ren, S. et al. 2011. Laboratory Assessment and Field Pilot of Near Miscible CO₂ Injection for IOR and Storage in a Tight Oil Reservoir of Shengli Oilfield China. Paper presented at the SPE Enhanced Oil Recovery Conference, Kuala Lumpur, Malaysia, 10–20 July. SPE-144108-MS. https://doi.org/10.2118/144108-MS.
- Sebastian, H. M. and Lawrence, D. D. 1992. Nitrogen Minimum Miscibility Pressures. Paper presented at the SPE/DOE Enhanced Oil Recovery Symposium, Tulsa, Oklahoma, USA, 22–24 April. SPE-24134-MS. https://doi.org/10.2118/24134-MS.
- Shen, Z. and Sheng, J. J. 2016. Experimental Study of Asphaltene Aggregation during CO₂ and CH₄ Injection in Shale Oil Reservoirs. Paper presented at the SPE Improved Oil Recovery Conference, Tulsa, Oklahoma, USA, 11–13 April. SPE-179675-MS. https://doi.org/10.2118/179675-MS.
- Shen, Z. and Sheng, J. J. 2017. Experimental Study of Permeability Reduction and Pore Size Distribution Change due to Asphaltene Deposition during CO₂ Huff and Puff Injection in Eagle Ford Shale. *Asia-Pac J Chem Eng* 12 (3): 381–390. https://doi.org/10.1002/apj.2080.
- Speight, J. G. 2014. The Chemistry and Technology of Petroleum. Boca Raton, Florida, USA: CRC Press.
- Su, H., Zhou, F., Wang, Q. et al. 2021. An Integrated Simulation Approach To Predict Permeability Impairment under Simultaneous Aggregation and Deposition of Asphaltene Particles. SPE J. 26 (4): 2231–2244. SPE-205381-PA. https://doi.org/10.2118/205381-PA.
- Vahidi, A. and Zargar, G. 2007. Sensitivity Analysis of Important Parameters Affecting Minimum Miscibility Pressure (MMP) of Nitrogen Injection into Conventional Oil Reservoirs. Paper presented at the SPE/EAGE Reservoir Characterization and Simulation Conference, Abu Dhabi, UAE, 28–31 October. SPE-111411-MS. https://doi.org/10.2118/111411-MS.
- Wang, P., Zhao, F., Hou, J. et al. 2018. Comparative Analysis of CO₂, N₂, and Gas Mixture Injection on Asphaltene Deposition Pressure in Reservoir Conditions. *Energies* 11 (9): 2483. https://doi.org/10.3390/en11092483.
- Yang, Z., Ma, C. F., Lin, X. S. et al. 1999. Experimental and Modeling Studies on the Asphaltene Precipitation in Degassed and Gas-Injected Reservoir Oils. Fluid Phase Equilibria 157 (1): 143–158. https://doi.org/10.1016/S0378-3812(99)00004-7.
- Yu, Y. and Sheng, J. J. 2015. An Experimental Investigation of the Effect of Pressure Depletion Rate on Oil Recovery from Shale Cores by Cyclic N₂ Injection. Paper presented at the Unconventional Resources Technology Conference, San Antonio, Texas, USA, 20–22 July. SPE-178494-MS. https://doi.org/10.2118/178494-MS.
- Zadeh, G. A., Moradi, S., Dabir, B. et al. 2011. Comprehensive Study of Asphaltene Precipitation due to Gas Injection: Experimental Investigation and Modeling. Paper presented at the SPE Enhanced Oil Recovery Conference, Kuala Lumpur, Malaysia, 19–20 July. SPE-143454-MS. https://doi.org/10.2118/143454-MS.
- Zendehboudi, S., Shafiei, A., Bahadori, A. et al. 2014. Asphaltene Precipitation and Deposition in Oil Reservoirs—Technical Aspects, Experimental and Hybrid Neural Network Predictive Tools. *Chem Eng Res Des* **92** (5): 857–875. https://doi.org/10.1016/j.cherd.2013.08.001.